

## Electronic Supplementary Information (ESI)

# **Homologous Co<sub>3</sub>O<sub>4</sub>||CoP nanowires grown on carbon cloth as a high-performance electrode pair for triclosan degradation and hydrogen evolution**

Chaojie Lyu,<sup>a</sup> Jinlong Zheng,<sup>#,a</sup> Rui Zhang,<sup>a</sup> Ruqiang Zou,<sup>b</sup> Bin Liu,<sup>c</sup> and Wei Zhou<sup>\*,a</sup>

<sup>a</sup>*School of Chemistry, Beihang University, Beijing 100191, China*

<sup>b</sup>*Beijing Key Laboratory for Theory and Technology of Advanced Battery Materials, Department of Materials Science and Engineering, College of Engineering, Peking University, Beijing 100871, China*

<sup>c</sup>*Institute for Food & Bioresource Engineering, College of Engineering, Peking University, Beijing 100871, China*

*#The author contributed equally to the first author.*

*E-mail:* zhouwei@buaa.edu.cn

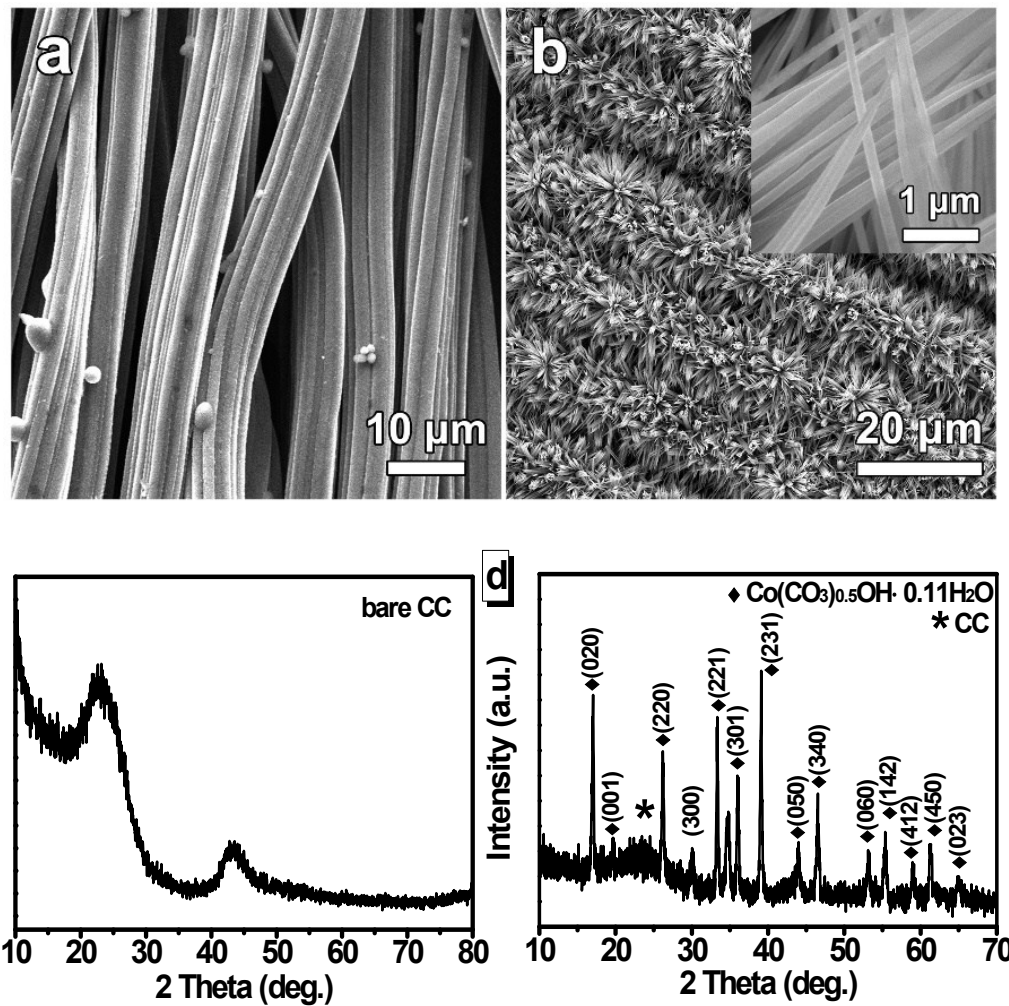


**Fig. S1** (a) SEM image of the bare carbon cloth (CC). (b) SEM image of the precursor/CC with magnified nanowires inserted, indicating the whole surface of the CC was uniformly coated with nanowires with diameters of 100-200 nm. (c, d) XRD patterns of the bare CC and the precursor/CC. The marked diffraction peaks of the Co precursor in Fig. S1d can be well indexed to  $\text{Co}(\text{CO}_3)_{0.5}\text{OH} \cdot 0.11\text{H}_2\text{O}$  (JCPDS No. 48-0083), in agreement with reported references. The peak marked with asterisk at  $\sim 24.5^\circ$  came from CC. [S1, S2]

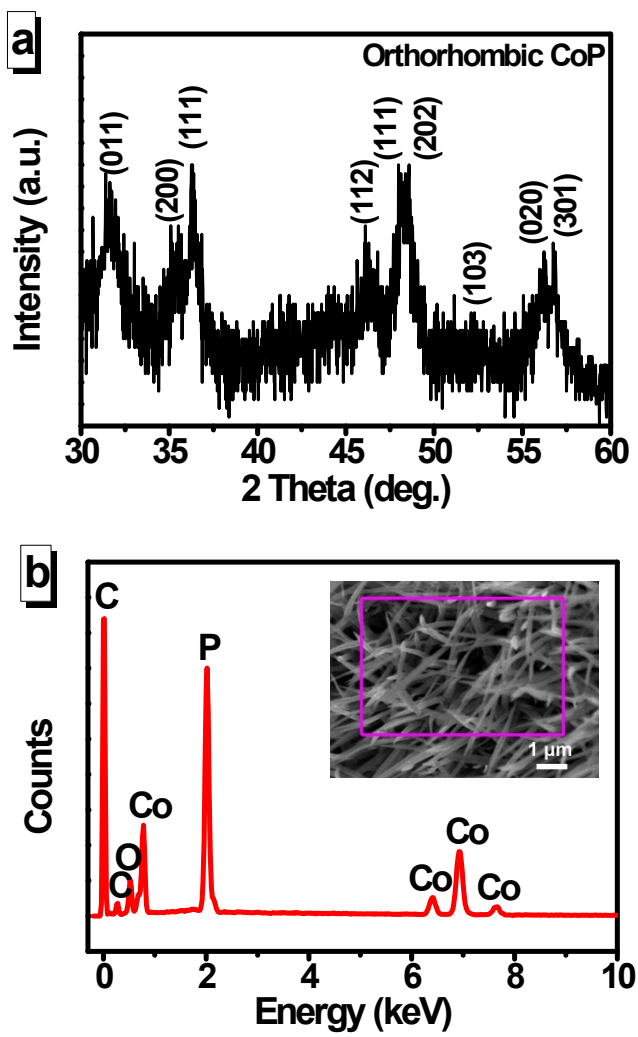


**Fig. S2** (a) XRD patterns of the CoP NWs/CC with these diffraction peaks corresponding to orthorhombic CoP (JCPDS No. 29-0497). (b) EDX spectrum of the CoP NWs/CC with the selected area inserted, revealing the existence of Co and P with atomic ratio of 1:1.2, in agreement with the result of XRD pattern.

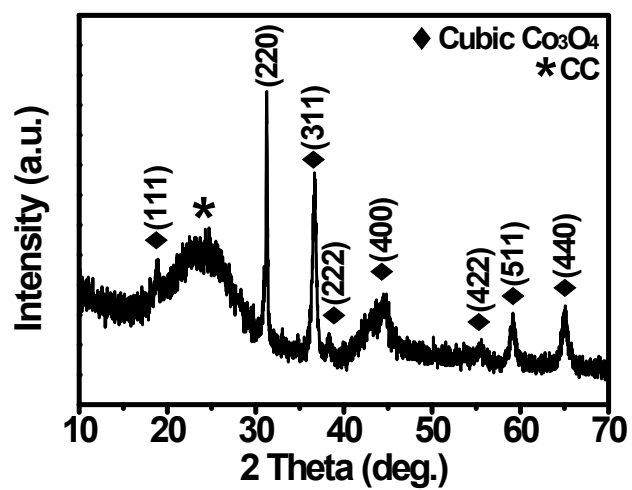


**Fig. S3** XRD pattern of the  $\text{Co}_3\text{O}_4$  NWs/CC, confirming the heat-treated product was transformed to cubic  $\text{Co}_3\text{O}_4$  (JCPDS No. 43-1003). The peak marked with asterisk at  $\sim 24.5^\circ$  came from CC.

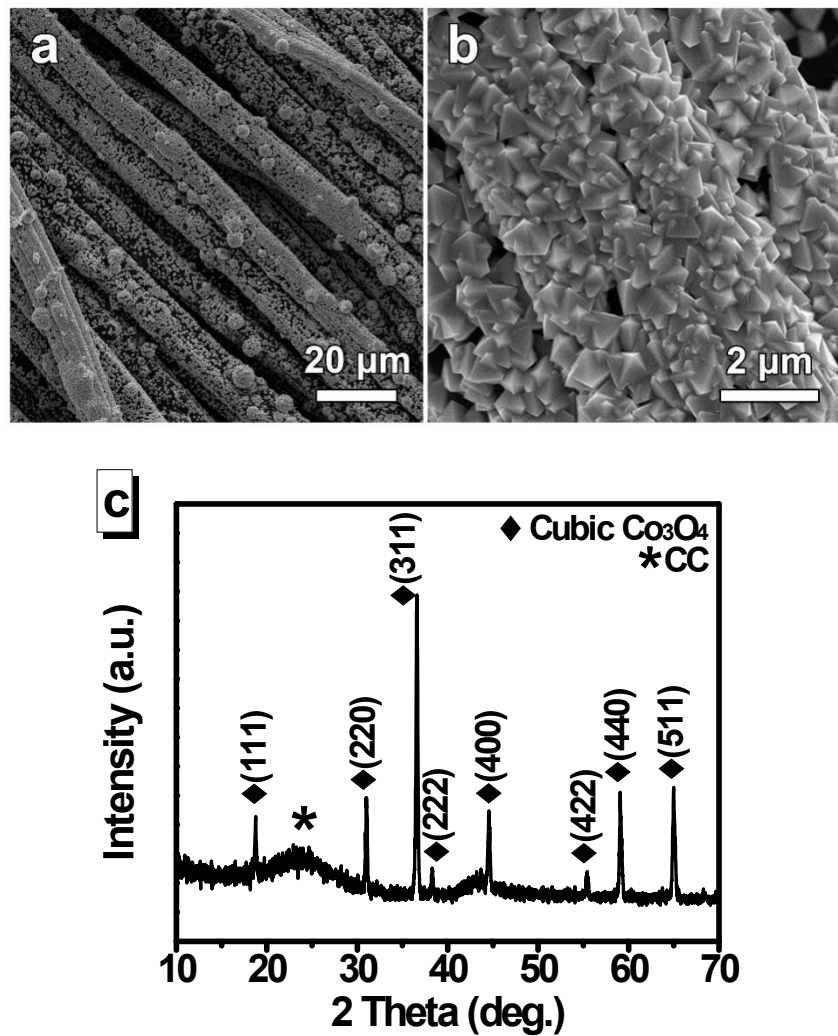


**Fig. S4** (a, b) Low- and high-magnification SEM images of the  $\text{Co}_3\text{O}_4$  Oct/CC, showing the octahedron with an average size of  $\sim 500 \text{ nm}$ . (c) XRD pattern of the  $\text{Co}_3\text{O}_4$  Oct/CC. All the diffraction peaks could be indexed well with standard cubic  $\text{Co}_3\text{O}_4$  (JCPDS No. 43-1003). The peak marked with asterisk at  $\sim 24.5^\circ$  came from CC.

**Table S1** Comparison of HER performance in 0.5 M H<sub>2</sub>SO<sub>4</sub> (pH=0), 1 M PBS (pH =7), and 1 M KOH (pH=14) for CoP NWs/CC with other Co-based Electrocatalysts.

<b>pH = 0</b>				
Catalyst	Electrolyte	$\eta$ (mV) @ 10 mA cm <sup>-2</sup>	Tafel slope (mV dec <sup>-1</sup> )	Reference
Co <sub>9</sub> S <sub>8</sub> /NC@MoS <sub>2</sub>	0.5 M H <sub>2</sub> SO <sub>4</sub>	117	68.8	<i>ACS Appl. Mater. Inter.</i> 2017, <b>9</b> , 28394-28405 [S3]
CoSe <sub>2</sub> @G	0.5 M H <sub>2</sub> SO <sub>4</sub>	210	42	<i>Chem. Eng. J.</i> 2017, <b>321</b> , 105-112 [S4]
CoP NPs@NPC	0.5 M H <sub>2</sub> SO <sub>4</sub>	134	79	<i>Nanoscale</i> , 2017, <b>9</b> , 3555-3560 [S5]
Ni <sub>2</sub> P/NiCoP@NCCs	0.5 M H <sub>2</sub> SO <sub>4</sub>	136	79	<i>J. Mater. Chem. A</i> , 2017, <b>5</b> , 16568-16572 [S6]
CoP NRs	0.5 M H <sub>2</sub> SO <sub>4</sub>	123	63	<i>Mater. Lett.</i> , 2017, <b>202</b> , 146-149 [S7]
Co <sub>2</sub> P	0.5 M H <sub>2</sub> SO <sub>4</sub>	240	76	<i>Nano Lett.</i> , 2016, <b>16</b> , 4691-4698 [S8]
CoP-Co	0.5 M H <sub>2</sub> SO <sub>4</sub>	135	66	<i>ACS Nano</i> , 2017, <b>11</b> , 4358-4364 [S9]
CoP NWs/CC	0.5 M H <sub>2</sub> SO <sub>4</sub>	119	73	<b>Our Work</b>

<b>pH = 7</b>				
Catalyst	Electrolyte	$\eta$ (mV) @ 10 mA cm <sup>-2</sup>	Tafel slope (mV dec <sup>-1</sup> )	Reference
CoO/CoSe <sub>2</sub>	1 M PBS	450	131	<i>Adv. Sci.</i> 2016, <b>3</b> , 1500426 [S10]
Co <sub>2</sub> N/TM	1 M PBS	290	138	<i>Catal. Sci. Technol.</i> , 2017, <b>7</b> , 2689-2694 [S11]

Co <sub>9</sub> S <sub>8</sub> /CC	1 M PBS	175	\	<i>J. Mater. Chem. A</i> , 2016, <b>4</b> , 6860-6867 [S12]
Ni–Co–S	1 M PBS	280	73	<i>ACS Appl. Mater. Inter.</i> 2017, <b>9</b> , 19746-19755 [S13]
Co-B	1 M PBS	251	75	<i>J. Power Sources</i> , 2015, <b>279</b> , 620-625 [S14]
CoP NPs@NPC	1 M PBS	423	268	<i>Nanoscale</i> , 2017, <b>9</b> , 3555-3560 [S5]
CoP NWs/CC	1 M PBS	130	144	<b>Our Work</b>

**pH = 14**

Catalyst	Electrolyte	$\eta$ (mV) @ 10 mA cm <sup>-2</sup>	Tafel slope (mV dec <sup>-1</sup> )	Potential Rention Rate (Testing time)	Reference
Co@NC/NF	0.1 M KOH	240	\	92(45h)	<i>ChemElectroChem</i> , 2017, <b>4</b> , 188-193 [S15]
NiCo HNSs	1 M KOH	230	87.5	78.2(5h)	<i>J. Mater. Chem. A</i> , 2017, <b>5</b> , 7769-7775 [S16]
Co–Ni–B	1 M KOH	205	\	90(12h)	<i>J. Mater. Chem. A</i> , 2017, <b>5</b> , 12379-12384 [S17]
Co <sub>4</sub> Mo <sub>2</sub> @NC	1 M KOH	218	73.5	75(13h)	<i>J. Mater. Chem. A</i> , 2017, <b>5</b> , 16929-16935 [S18]
CoMnCH	1 M KOH	180	\	96.7(10h)	<i>J. Am. Chem. Soc.</i> 2017, <b>139</b> , 8320-8328 [S19]
CoP	1 M KOH	139	70.3	77.5(10h)	<i>Nano Energy</i> , 2017, <b>38</b> , 290-296 [S20]

Ni–Co–Ti	1 M KOH	106	41	88(150h)	<i>ACS Appl. Mater. Inter.</i> , 2017, <b>9</b> , 12416-12426 [S21]
Ce-CoP	1 M KOH	92	63.5	93.1(10h)	<i>Nano Energy</i> , 2017, <b>38</b> , 290-296 [S20]
CoP NWs/CC	1 M KOH	69	70	98.5% (24h)	<b>Our Work</b>

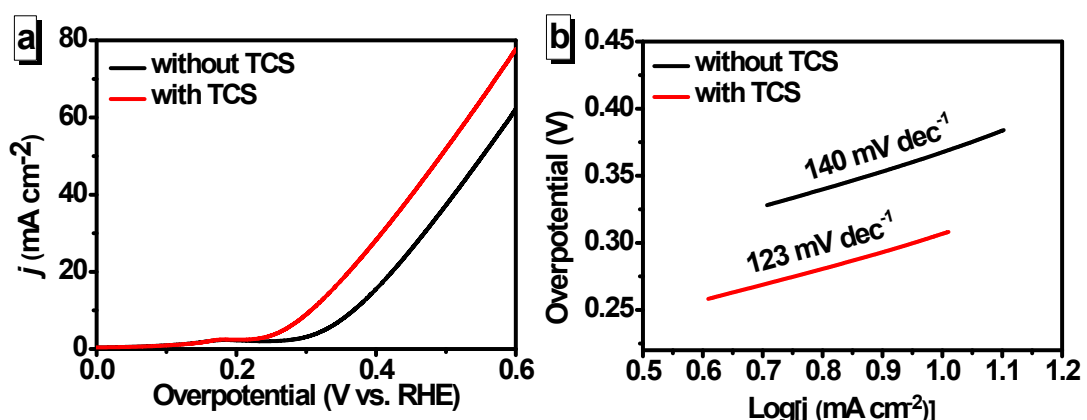


**Fig. S5** (a) LSV curves of  $\text{Co}_3\text{O}_4$  NWs/CC at a scan rate of  $2 \text{ mV s}^{-1}$  in 1 M KOH with and without TCS. (b) Corresponding Tafel plots of  $\text{Co}_3\text{O}_4$  NWs/CC in 1 M KOH with and without TCS.

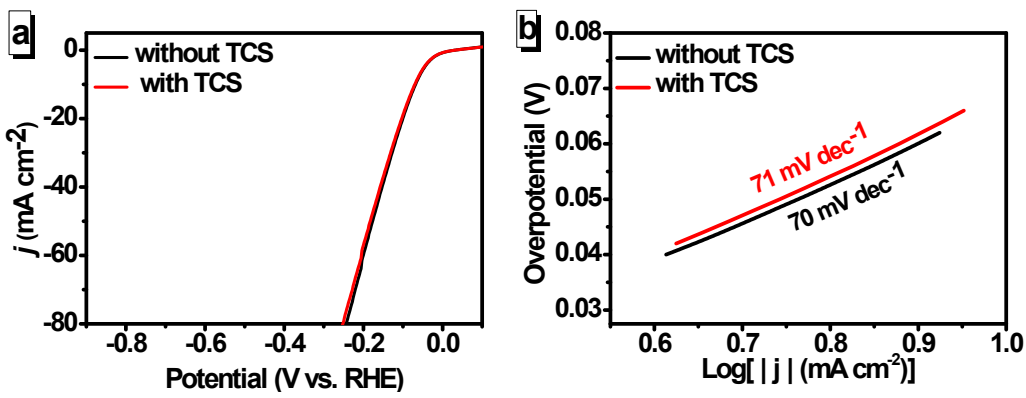


**Fig. S6** (a) LSV curves of CoP NWs/CC for HER at a scan rate of  $2 \text{ mV s}^{-1}$  in  $1 \text{ M KOH}$  with and without TCS. (b) Corresponding Tafel plots of CoP NWs/CC in  $1 \text{ M KOH}$  with and without TCS.

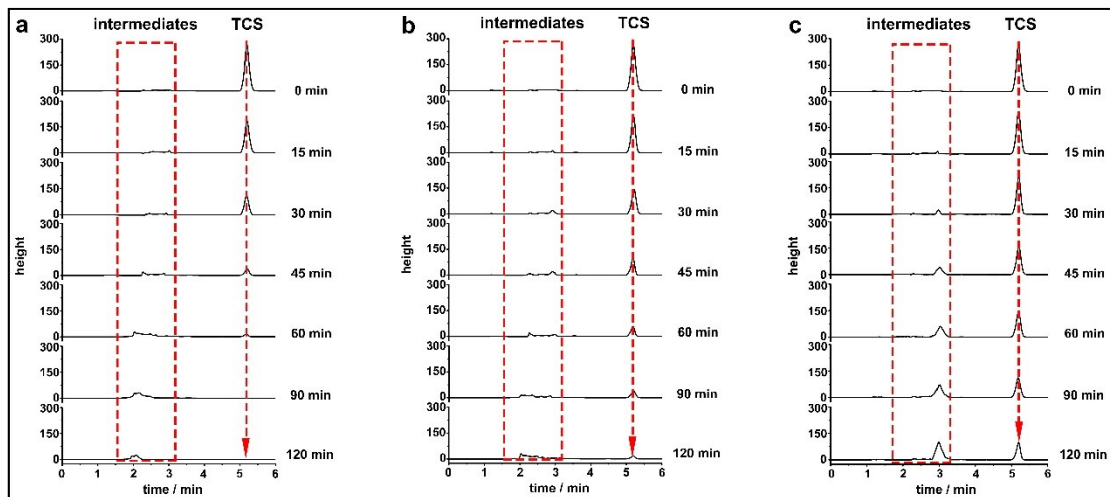


**Fig. S7** Retention time of TCS solution ( $40 \text{ mg L}^{-1}$ ) and its intermediates during the electrochemical degradation process, using (a) the  $\text{Co}_3\text{O}_4$  NWs/CC||CoP NWs/CC pair, (b) the  $\text{Co}_3\text{O}_4$  Oct/CC||CoP NWs/CC pair, and (c) the CC||CoP NWs/CC pair. Obviously, the peaks with retention time of  $\sim 5.2 \text{ min}$  correspond to TCS while the peaks with retention time between 2 and 3 min correspond to the intermediates. Obviously, the rapid peak decrease of TCS using  $\text{Co}_3\text{O}_4$  NWs/CC suggested its fast degradation rate.

**Table S2** Comparison of TCS degradation with other literatures.

Electrode	TCS concentration (mg L <sup>-1</sup> )	Current density (mA cm <sup>-2</sup> )	Time (min)	Degradation Rates (%)	Reference
boron-doped diamond (BDD)	1.19	28.5	180	62	<i>J. Electroanal. Chem.</i> , 2016, <b>776</b> , 148-151 [S22]
Ti/SnO <sub>2</sub> -Sb/Ce-PbO <sub>2</sub>	4	10	5	99.9	<i>CLEAN-Soil, Air, Water.</i> , 2015, <b>43</b> , 958-966 [S23]
Ti/MMO	5	3	30	100	<i>Chemosphere</i> , 2013, <b>93</b> , 2796-2804 [S24]
p-Si-BDD	100	30	600	95	<i>Chem. Eng. Trans.</i> , 2014, <b>41</b> , 103-108 [S25]
Pt/carbon felt	5	13	10	100	<i>Electrochim. Acta.</i> , 2007, <b>52</b> , 5493-5503 [S26]
Co <sub>3</sub> O <sub>4</sub> NWs/CC	40	10	60	95	<b>Our work</b>

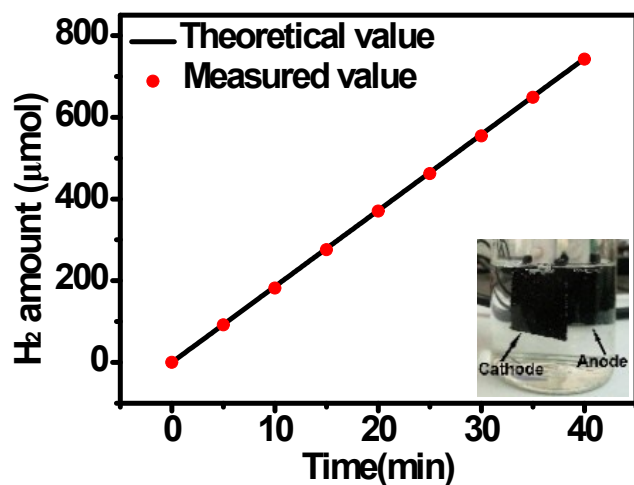


**Fig. S8** Measured H<sub>2</sub> quantity compared with theoretically calculated H<sub>2</sub> quantity *vs.* time for CoP NWs/CC.

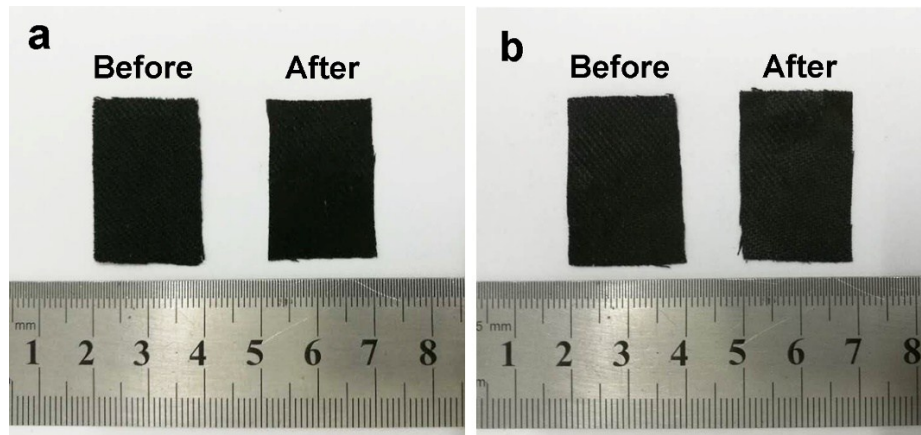


**Fig. S9** Optical photos of (a) CoP NWs/CC and (b) Co<sub>3</sub>O<sub>4</sub> NWs/CC electrodes before and after 6 successive electrolysis cycles.

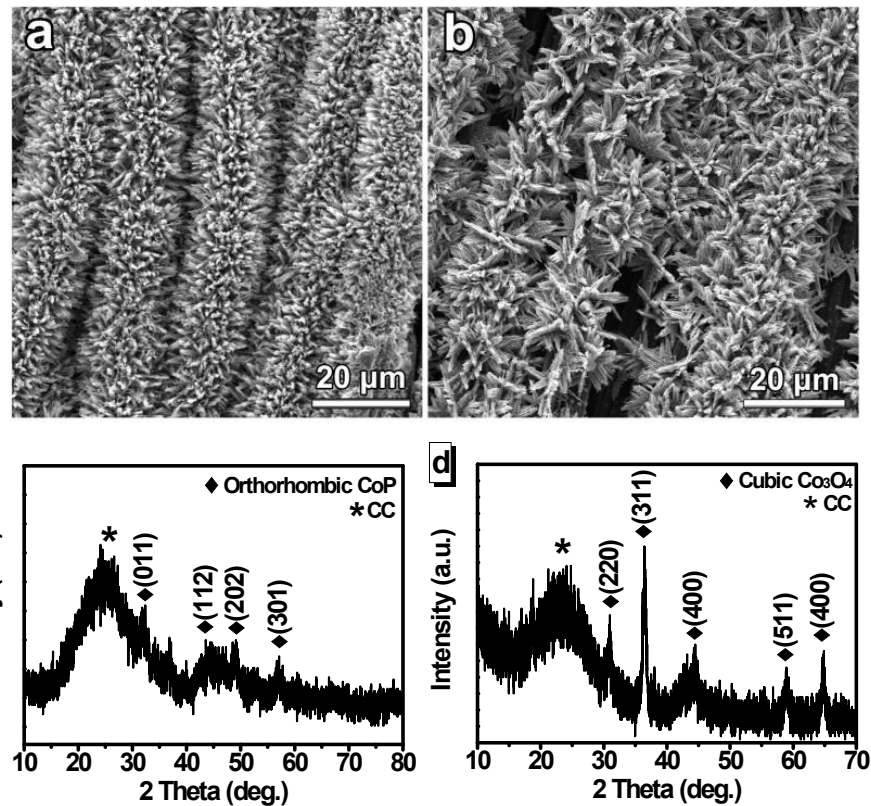


**Fig. S10** (a-b) SEM images of CoP NWs/CC and Co<sub>3</sub>O<sub>4</sub> NWs/CC after 6 successive electrolysis cycles. (c-d) XRD patterns of CoP NWs/CC and Co<sub>3</sub>O<sub>4</sub> NWs/CC after 6 successive electrolysis cycles. The peaks marked with asterisks at ~24.5° came from CC.

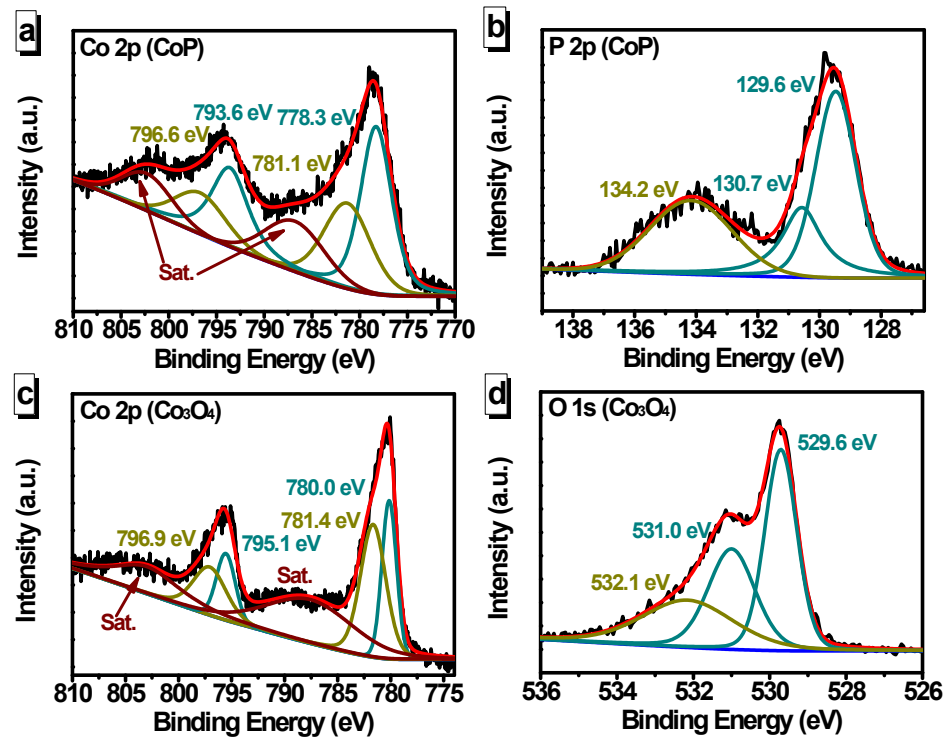


**Fig. S11** High-resolution XPS spectra of (a) Co 2p and (b) P 2p for CoP. High-resolution XPS spectra of (c) Co 2p and (d) O 1s for  $\text{Co}_3\text{O}_4$  after 6 successive electrolysis cycles.

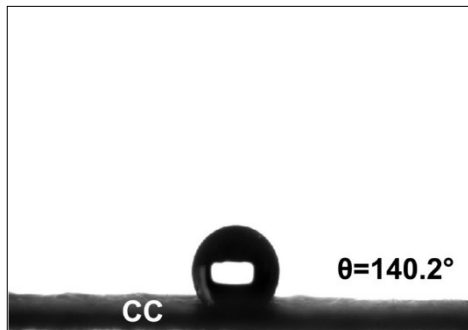


**Fig. S12** Wettability test of the bare CC without treatment with contact angle of about  $140.2^\circ$ , showing its very poor hydrophilicity.

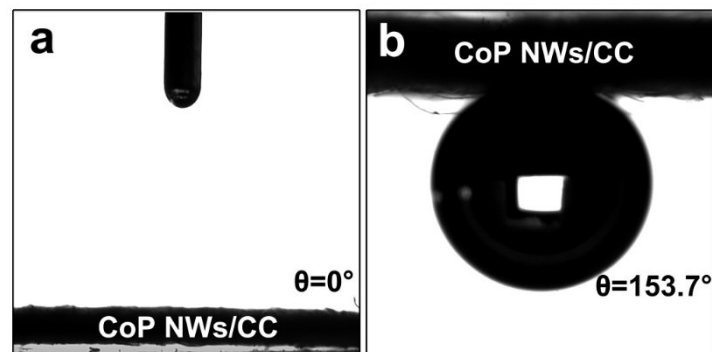


**Fig. S13** Wettability tests of the CoP NWs/CC to TCS solution. (a) Liquid contact angle of  $\sim 0^\circ$ , suggesting the surface of CoP NWs/CC was superhydrophilic. (b) Bubble contact angle of  $\sim 153.7^\circ$ . As the bubble contact is larger than  $150^\circ$ , the surface of CoP NWs/CC is considered to be “superaerophobic”.[S22, S23]

**Table S3** Electrolysis time and corresponding peak area of the triclosan degradation intermediates by Chronopotentiometry at 10 mA cm<sup>-2</sup>.

Identified intermediate compounds	Electrolysis time (min)	Peak area	Retention time (min)	Molecular weight (g/mol)
phenol	0	11.3		
	15	21.5		
	30	45.8		
	45	90.3	2.1	94.111
	60	163.2		
	90	148.9		
	120	79.5		
1,2-dihydroxybenzene	0	9.6		
	15	15.6		
	30	23.6		
	45	48.9	2.5	110.11
	60	31.2		
	90	12.4		
	120	0		
2-phenoxyphenol	0	12.5		
	15	50.6		
	30	39.8		
	45	10.3	3.0	186.22
	60	11.6		
	90	9.5		
	120	0		
triclosan	0	2542		
	15	1727		
	30	1012		
	45	340	5.2	289.54
	60	125		
	90	0		
	120	0		

## References

- (S1) H. Yang, Y. Zhang, F. Hu and Q. Wang, *Nano Lett.*, 2015, **15**, 7616-7620.
- (S2) L. Cui, D. Liu, S. Hao, F. Qu, G. Du, J. Liu, A. Asiri and X. Sun, *Nanoscale*, 2017, **9**, 3752-3756.
- (S3) H. Li, X. Qian, C. Xu, S. Huang, C. Zhu, X. Jiang, L. Shao and L. Hou, *ACS Appl. Mater.*

- Inter.*, 2017, **9**, 28394-28405.
- (S4) C. Dai, X. Tian, Y. Nie, C. Tian, C. Yang, Z. Zhou, Y. Li and X. Gao, *Chem. Eng. J.*, 2017, **321**, 105-112.
- (S5) Z. Pu, I. S. Amiinu, C. Zhang, M. Wang, Z. Kou and S. Mu, *Nanoscale*, 2017, **9**, 3555-3560.
- (S6) L. Han, T. Yu, W. Lei, W. Liu, K. Feng, Y. Ding, G. Jiang, P. Xu and Z. Chen, *J. Mater. Chem. A*, 2017, **5**, 16568-16572.
- (S7) J. Zhang, X. Liang, X. Wang and Z. Zhuang, *Mater. Lett.*, 2017, **202**, 146-149.
- (S8) M. Zhuang, X. Ou, Y. Dou, L. Zhang, Q. Zhang, R. Wu, Y. Ding, M. Shao and Z. Luo, *Nano Lett.*, 2016, **16**, 4691-4698.
- (S9) H. Wang, S. Min, Q. Wang, D. Li, G. Casillas, C. Ma, Y. Li, Z. Liu, L. J. Li, J. Yuan, M. Antonietti and T. Wu, *ACS Nano*, 2017, **11**, 4358-4364.
- (S10) K. Li, J. Zhang, R. Wu, Y. Yu, and B. Zhang, *Adv. Sci.*, 2016, **3**, 1500426.
- (S11) L. Zhang, L. Xie, M. Ma, F. Qu, G. Du, A. M. Asiri, L. Chen and X. Sun, *Catal. Sci. Technol.*, 2017, **7**, 2689-2694.
- (S12) L. Feng, M. Fan, Y. Wu, Y. Liu, G. Li, H. Chen, W. Chen, D. Wang and X. Zou, *J. Mater. Chem. A*, 2016, **4**, 6860-6867.
- (S13) A. Irshad, N. Munichandraiah, *ACS Appl. Mater. Inter.*, 2017, **9**, 19746-19755.
- (S14) S. Gupta, N. Patel, A. Miotello and D. Kothari, *J. Power Sources*, 2015, **279**, 620-625.
- (S15) A. Ajaz, J. Masa, C. Rcsler, W. Xia, P. Weide, R. A. Fischer, W. Schuhmann and M. Muhler, *ChemElectroChem*, 2017, **4**, 188-193.
- (S16) X. Sun, Q. Shao, Y. Pi, J. Guo and X. Huang, *J. Mater. Chem. A*, 2017, **5**, 7769-7775.
- (S17) N. Xu, G. Cao, Z. Chen, Q. Kang, H. Da and P. Wang, *J. Mater. Chem. A*, 2017, **5**, 12379-12384.
- (S18) J. Jiang, Q. Liu, C. Zeng and L. Ai, *J. Mater. Chem. A*, 2017, **5**, 16929-16935.
- (S19) T. Tang, W. Jiang, S. Niu, N. Liu, H. Luo, Y. Chen, S. Jin, F. Gao, L. Wan, and J. Hu, *J. Am. Chem. Soc.*, 2017, **139**, 8320-8328.
- (S20) W. Gao, M. Yana, H. Y. Cheung, Z. Xia, X. Zhou, Y. Qin, C. Y. Wong, J. C. Hob, C. Chang and Y. Qu, *Nano Energy*, 2017, **38**, 290-296.
- (S21) P. Ganesan, A. Sivanantham and S. Shanmugam, *ACS Appl. Mater. Inter.*, 2017, **9**, 12416-12426.
- (S22) J. A. Barrios, A. Cano, J. E. Becerril and B. Jiménez, *J. Electroanal. Chem.*, 2016, **776**, 148-151.
- (S23) D. Maharana, J. Niu, N. N. Rao, Z. Xu and J. Shi, *CLEAN-Soil, Air, Water.*, 2015, **43**, 958-966.
- (S24) S. Yuan, N. Gou, A. N. Alshawabkeh and A. Z. Gu, *Chemosphere.*, 2013, **93**, 2796-2804.
- (S25) C. Sáez, M. J. M. Vidales, P. Cañizares and S. Cotillas, *Chem. Eng. Trans.*, 2014, **41**, 103-108.
- (S26) I. Sirés, N. Oturan, M. A. Oturan, R. M. Rodríguez, J. A. Garrido and E. Brillas, *Electrochim Acta.*, 2007, **52**, 5493-5503.